

Supplementary Information: QM and ONIOM Studies on Thermally Activated Delayed Fluorescence of Copper(I) Complexes in Gas Phase, Solution, and Crystal

Yuan-Jun Gao, Wen-Kai Chen, Zi-Rui Wang, Wei-Hai Fang, and Ganglong Cui*

Key Laboratory of Theoretical and Computational Photochemistry, Ministry of Education,
Chemistry College, Beijing Normal University, Beijing 100875, P. R. China

E-mail: ganglong.cui@bnu.edu.cn

Table of Contents

1. **Table S1.** Key geometric parameters of complexes **1** and **2** in the gas phase, solution, and crystal (length in Å and angles in °).S3
2. **Table S2.** Key geometric parameters of ground state structures optimized by different basis sets for complexes **1** in crystal (length in Å and angles in °).S4
3. **Figure S1.** Key geometric parameters at the equilibrium geometries of the S_0 , S_1 , and T_1 states for **2** in the gas phase, solution and crystal. Left: bond lengths (in Å) for Cu-N1, Cu-N2, Cu-P1 and Cu-P2. Right: angles N1-Cu-N2 (θ_1), P1-Cu-P2 (θ_2), dihedral angle between N-Cu-N and P-Cu-P planes (θ_3) and N1-C1-C2-N2 (θ_4).S5
4. **Figure S2.** Schematic representations of the **1** (left) and **2** (right) clusters.S5
5. **Figure S3.** Overlays of S_0 structures in the gas phase (green), solution (THF, blue) and crystal (red) for **1** and **2**. Overlays of S_1 and T_1 structures in the gas phase, solution and crystal also show in Figure S2, respectively.S6
6. **Figure S4.** Overlays of optimized S_0 structures (red) and X-Ray structures (silver) in crystal for compound **1** (left) and **2** (right).S6
7. **Figure S5.** TD-DFT computed absorption and emission spectra at the S_0 and S_1 minima in gas phase (green lines), solution (blue lines), and crystal (red lines) of compound **2**. Also shown are experimentally measured absorption (in solution, dotted lines) and emission spectra (in crystal phase, dotted lines).S7
8. **Figure S6.** (**1** left and **2** right) Absorption spectra (THF) are show in blue line and spectral envelope plotted with Gaussians of 1500 cm^{-1} full width at half-maximum are show in maroon dash line. The data points of the experimental spectrum are show in black dotted line.S7
9. **Figure S7.** TD-DFT computed absorption in gas phase (green lines), dichloromethane (blue lines), and crystal (red lines) of compound **1** and **2**. Also shown are experimentally measured absorption (in dichloromethane, dotted lines).S7
10. **Figure S8.** Adiabatic energy differences and reorganization energy calculated based on optimized S_1 and T_1 minima in gas, solution and crystal for **2**.S8

11. Figure S9. The temperature dependence of the interconversion and decay rates from 200 to 300 K for 2 .	S8
12. Figure S10. (R)ISC rate constant as a function of energy gap at different temperatures of 1 in gas, solution and crystal.	S9
13. Figure S11. (R)ISC rate constant as a function of energy gap at different temperatures of 2 in gas, solution and crystal.	S10
14. Figure S12. Huang-Rhys factors for energy conversion between S_1 and T_1 as well as displacement vectors of important vibration modes with the largest value of Huang-Rhys factor in gas, solution and crystal for 2 .	S11
15. Table S3. Relative energies (eV) of B3LYP/6-31G* & LANL2DZ (Cu) optimized structures for 1 and 2 in the gas phase, solution, and crystal. (Ground state energy as reference point).	S12
16. Table S4. Spin-orbit coupling matrix elements (SOCMEs) values, Marcus reorganization energy, intersystem crossing rates and reverse intersystem crossing rates (ISC from S_1 to T_1 and RISC from T_1 to S_1).	S13
17. Table S5. The temperature dependence of the intersystem crossing rates and reverse intersystem crossing rates (s^{-1}) (ISC from S_1 to T_1 and RISC from T_1 to S_1).	S14
18. Table S6. Oscillator strength, radiative rate constant and lifetime.	S15
19. Table S7. Vertical excitation energies, oscillator strengths, wavelength and singly occupied orbitals involved in the $S_0 \rightarrow S_n$ electronic transitions in the gas phase, solution, and crystal, which are computed by TD-B3LYP.	S16
20. Table S8. Vertical emission energies, oscillator strengths, wavelength and singly occupied orbitals involved in the $S_1 \rightarrow S_0$ and $T_1 \rightarrow S_0$ electronic transitions in the gas phase, solution, and crystal.	S22
21. Figure S13. Molecular orbitals at the S_0 , S_1 and T_1 minima of compound 1 in gas phase.	S23
22. Figure S14. Molecular orbitals at the S_0 , S_1 and T_1 minima of compound 1 in solution.	S24
23. Figure S15. Molecular orbitals at the S_0 , S_1 and T_1 minima of compound 1 in crystal.	S25
24. Figure S16. Molecular orbitals at the S_0 , S_1 and T_1 minima of compound 2 in gas phase.	S26
25. Figure S17. Molecular orbitals at the S_0 , S_1 and T_1 minima of compound 2 in solution.	S27
26. Figure S18. Molecular orbitals at the S_0 , S_1 and T_1 minima of compound 2 in crystal.	S28
27. Figure S19. Natural transition orbital pairs at the S_1 and T_1 minima for Compound 1 and 2 .	S29
28. Figure S20. TD-DFT computed HOMO and LUMO at the S_1 minima of compound 1 in solution.	S29
29. Figure S21. Overlays of S_1 (gray) and T_1 (green) structures in solution for complex 1 .	S30

Table S1. Key Geometric Parameters of Complexes **1** and **2** in the Gas Phase, Solution, and Crystal (Length in Å and Angles in °).

Gas				
Lengths	Cu-N1	Cu-N2	Cu-P1	Cu-P2
1-S₀	2.243	2.072	2.360	2.392
1-S₁	2.027	1.975	2.531	2.478
1-T₁	2.007	1.979	2.511	2.472
2-S₀	2.243	2.075	2.365	2.387
2-S₁	2.028	1.974	2.530	2.478
2-T₁	2.008	1.978	2.509	2.475
Angles	θ₁	θ₂	θ₃	θ₄
1-S₀	79.0	115.6	85.8	-0.1
1-S₁	83.4	106.7	58.9	11.1
1-T₁	83.1	107.8	61.2	4.7
2-S₀	78.9	115.9	86.2	-0.0
2-S₁	83.4	106.5	58.4	11.2
2-T₁	83.1	107.6	60.4	4.5
Solution				
Lengths	Cu-N1	Cu-N2	Cu-P1	Cu-P2
1-S₀	2.227	2.102	2.367	2.394
1-S₁	2.030	2.007	2.513	2.479
1-T₁	2.009	2.009	2.500	2.470
2-S₀	2.228	2.102	2.366	2.395
2-S₁	2.029	2.010	2.522	2.483
2-T₁	2.009	2.010	2.504	2.475
Angles	θ₁	θ₂	θ₃	θ₄
1-S₀	78.6	115.6	86.5	-0.5
1-S₁	82.8	106.3	55.3	10.6
1-T₁	82.5	107.5	57.6	4.0
2-S₀	78.6	115.4	86.8	-0.5
2-S₁	82.7	105.9	55.0	10.3
2-T₁	82.6	107.1	57.9	4.2
Crystal				
Lengths	Cu-N1	Cu-N2	Cu-P1	Cu-P2
1-S₀	2.143	2.087	2.327	2.348
1-S₁	2.001	1.994	2.437	2.440
1-T₁	1.979	1.994	2.420	2.439

2-S₀	2.173	2.085	2.326	2.412
2-S₁	2.026	2.003	2.430	2.483
2-T₁	2.002	1.999	2.429	2.499
Angles	θ₁	θ₂	θ₃	θ₄
1-S₀	79.6	116.2	83.3	1.3
1-S₁	83.4	108.8	68.1	17.8
1-T₁	83.1	109.9	70.9	12.7
2-S₀	79.0	116.7	87.8	10.4
2-S₁	83.4	108.6	75.1	21.1
2-T₁	83.1	109.7	76.9	17.7

Note: N1-Cu-N2 (θ_1), P1-Cu-P2 (θ_2), dihedral angle between N-Cu-N and P-Cu-P planes (θ_3) and N1-C1-C2-N2 (θ_4).

Table S2. Key Geometric Parameters of Ground State Structures Optimized by Different Basis Sets (with Same Functional B3LYP) for Complexes **1** in Crystal (Length in Å and Angles in °).

Crystal				
Lengths	Cu-N1	Cu-N2	Cu-P1	Cu-P2
6-31G* & LANL2DZ(Cu)	2.143	2.087	2.327	2.348
6-31G** & LANL2TZ-f(Cu)	2.123	2.069	2.302	2.320
6-31G* & 6-31+G*(P) & SDD(Cu)	2.126	2.072	2.280	2.300
Angles	θ₁	θ₂	θ₃	θ₄
6-31G* & LANL2DZ(Cu)	79.6	116.2	83.3	1.3
6-31G** & LANL2TZ-f(Cu)	80.0	116.4	80.0	0.6
6-31G* & 6-31+G*(P) & SDD(Cu)	79.8	117.0	83.4	0.5

Note: N1-Cu-N2 (θ_1), P1-Cu-P2 (θ_2), dihedral angle between N-Cu-N and P-Cu-P planes (θ_3) and N1-C1-C2-N2 (θ_4).

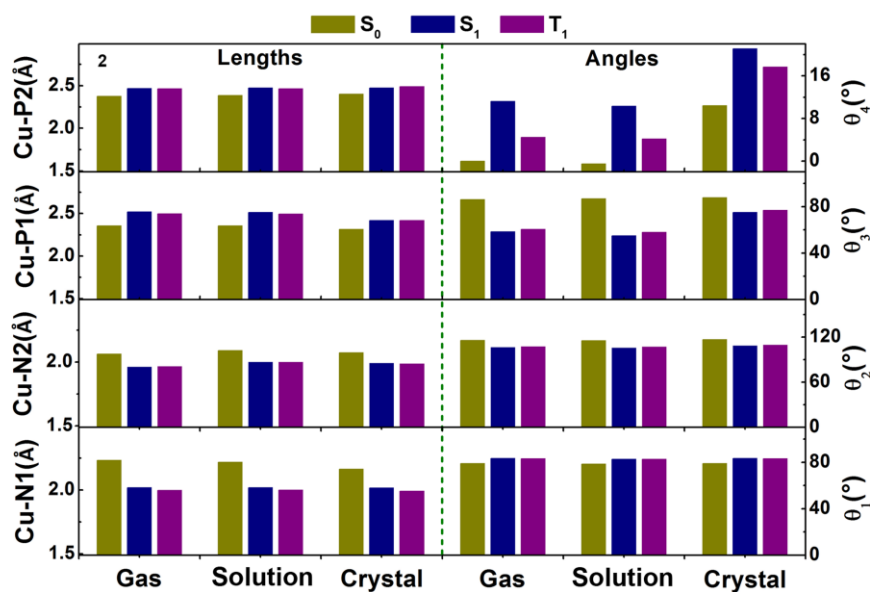


Figure S1. Key geometric parameters at the equilibrium geometries of the S₀, S₁, and T₁ states for **2** in the gas phase, solution and crystal. Left: bond lengths (in Å) for Cu-N1, Cu-N2, Cu-P1 and Cu-P2. Right: angles N1-Cu-N2 (θ_1), P1-Cu-P2 (θ_2), dihedral angle between N-Cu-N and P-Cu-P planes (θ_3) and N1-C1-C2-N2 (θ_4).

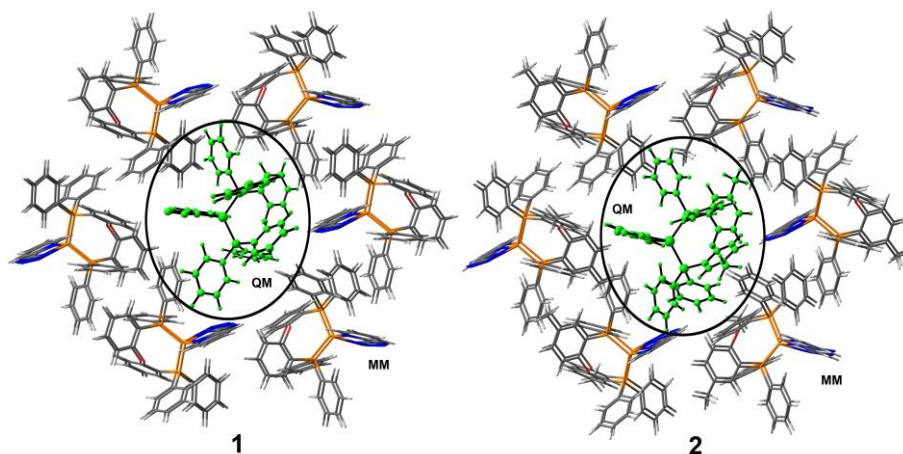


Figure S2. Schematic representations of clusters of compounds **1** (left) and **2** (right). The central monomer is treated at QM level and the outer monomers are treated at MM level.

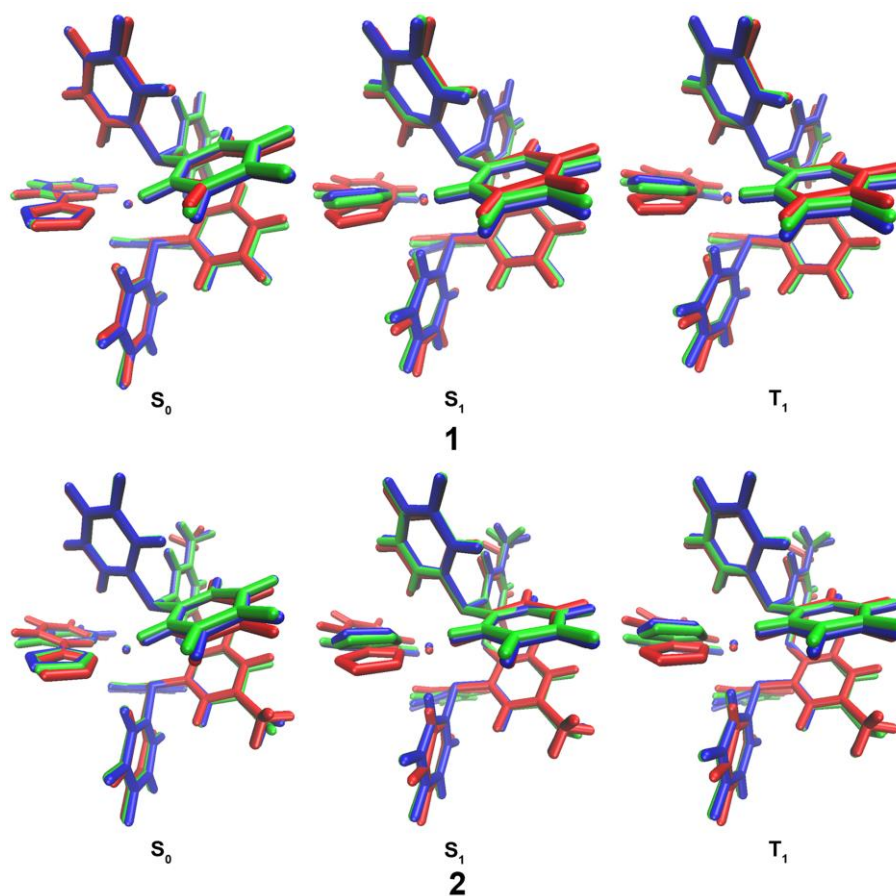


Figure S3. Overlays of S_0 , S_1 and T_1 structures in gas phase (green), solution (THF, blue) and crystal (red) for **1** and **2**, respectively.

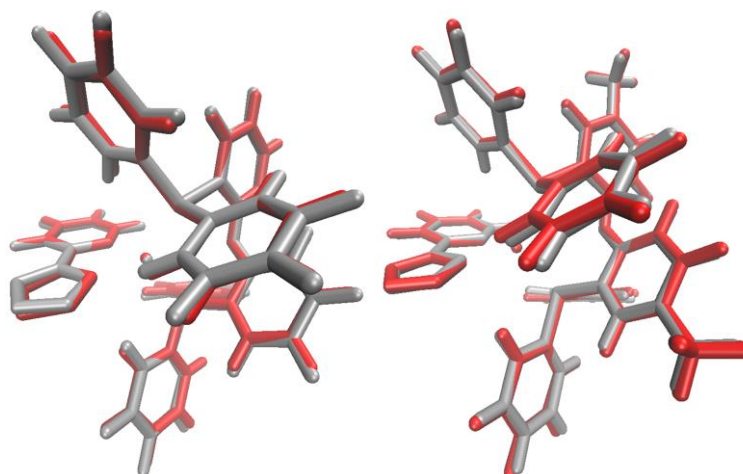


Figure S4. Overlays of optimized S_0 structures (red) and X-Ray structures (silver) in crystal for compound **1** (left) and **2** (right).

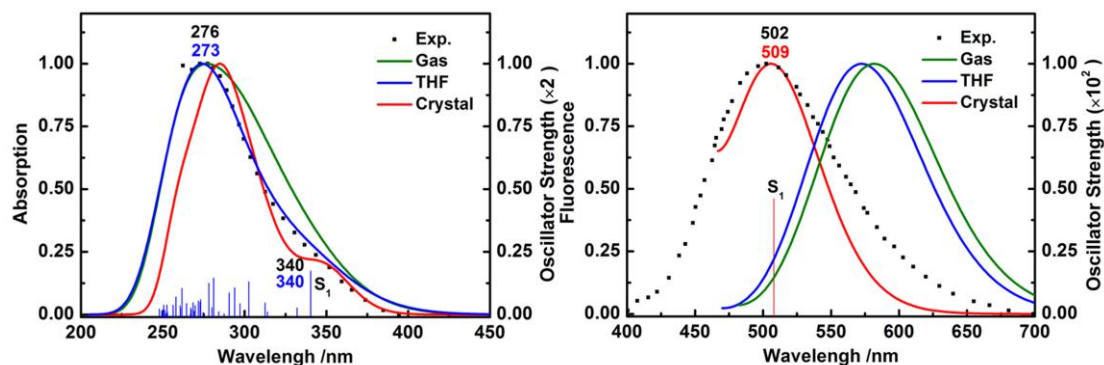


Figure S5. TD-DFT computed absorption and emission spectra at the S_0 and S_1 minima in gas phase (green lines), THF (blue lines), and crystal (red lines) of compound **2**. Also shown are experimentally measured absorption (in dichloromethane, dotted lines) and emission spectra (in the solid state, dotted lines).¹

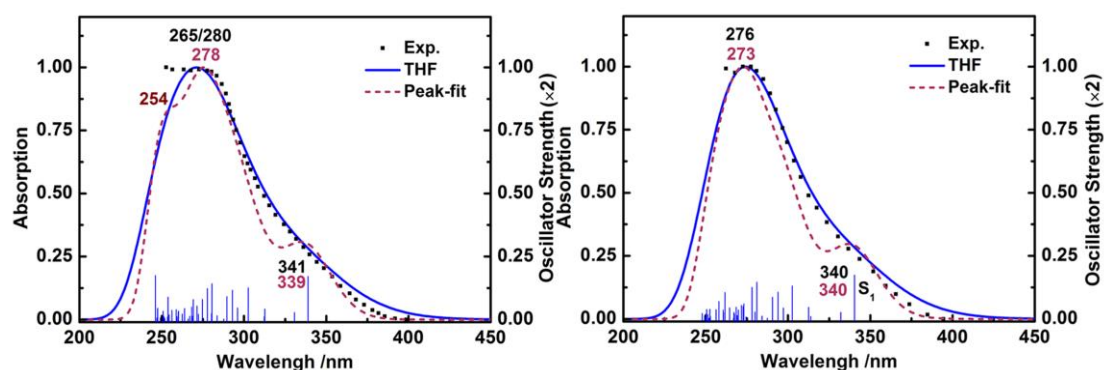


Figure S6. (1 left and 2 right) Absorption spectra (THF) are show in blue line and spectral envelope plotted with Gaussians of 1500 cm^{-1} full width at half-maximum are show in maroon dash line. The data points of the experimental spectrum are show in black dotted line.

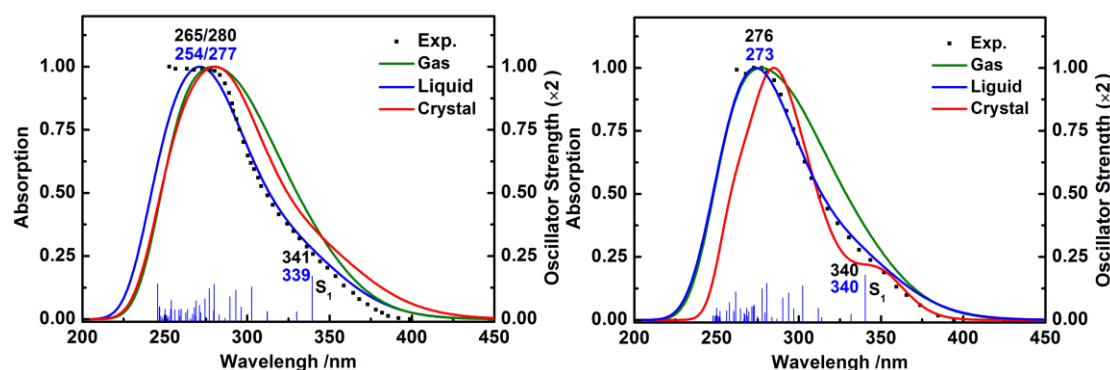


Figure S7. TD-DFT computed absorption in gas phase (green lines), dichloromethane (blue lines), and crystal (red lines) of compound **1** and **2**. Also shown are experimentally measured absorption (in dichloromethane, dotted lines).¹

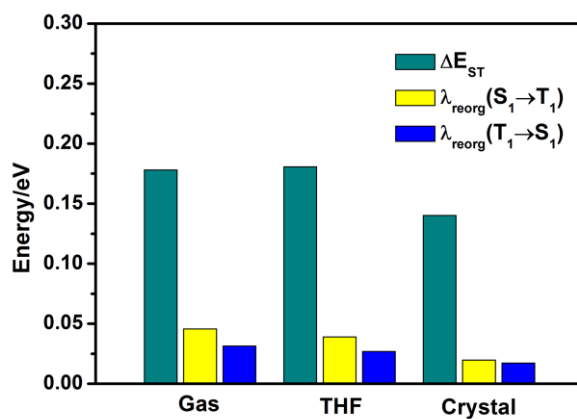


Figure S8. Adiabatic energy differences ($\Delta E_{S_1-T_1}$) and reorganization energy calculated based on optimized S_1 and T_1 minima (λ_{reorg}) in gas, solution and crystal for **2**.

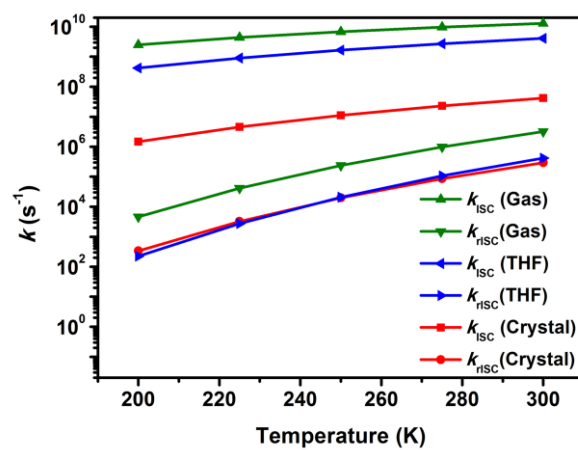


Figure S9. The temperature dependence of the interconversion and decay rates from 200 to 300 K for **2**.

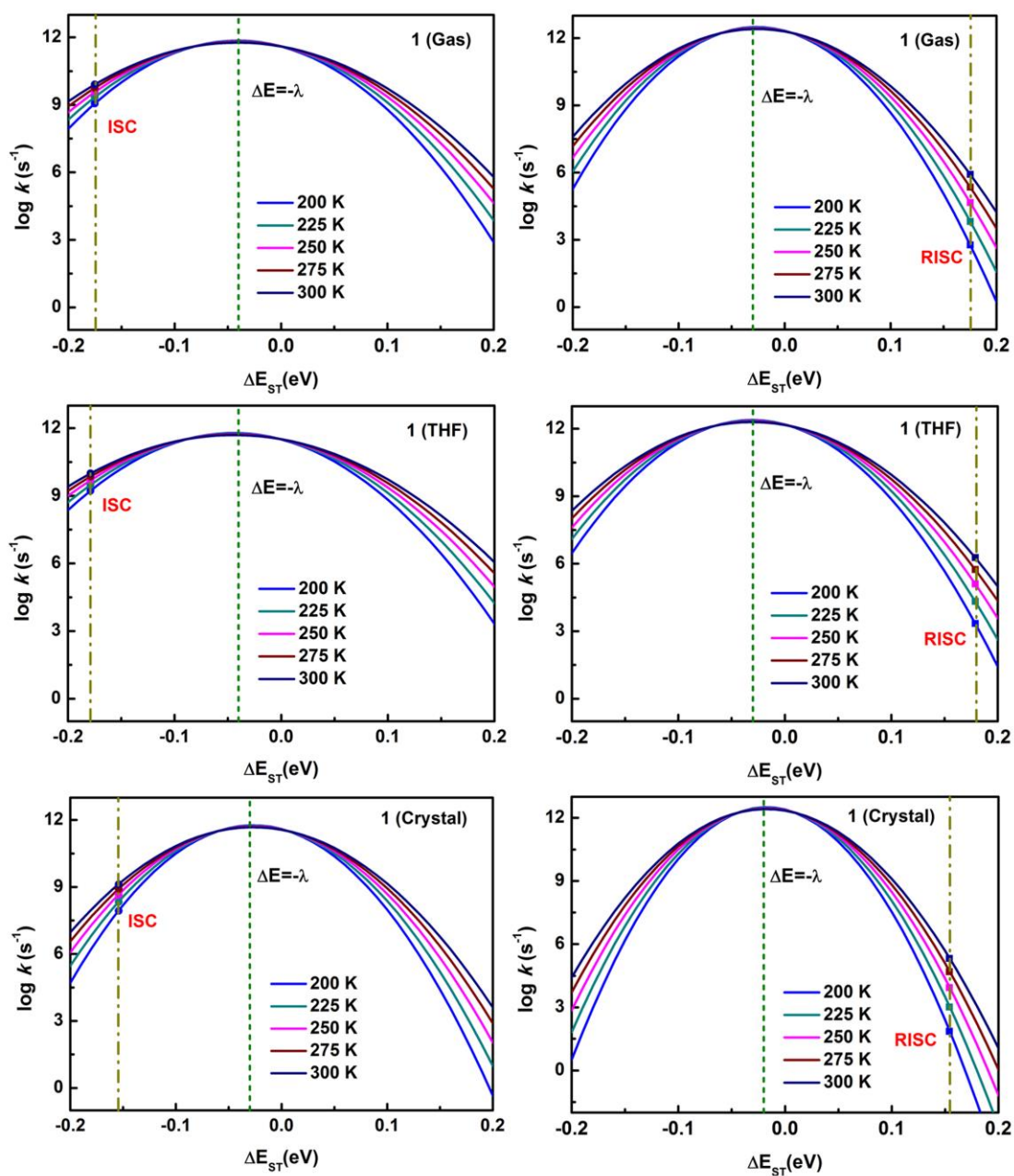


Figure S10. (R)ISC rate constant as a function of energy gap at different temperatures of **1** in gas, solution and crystal.

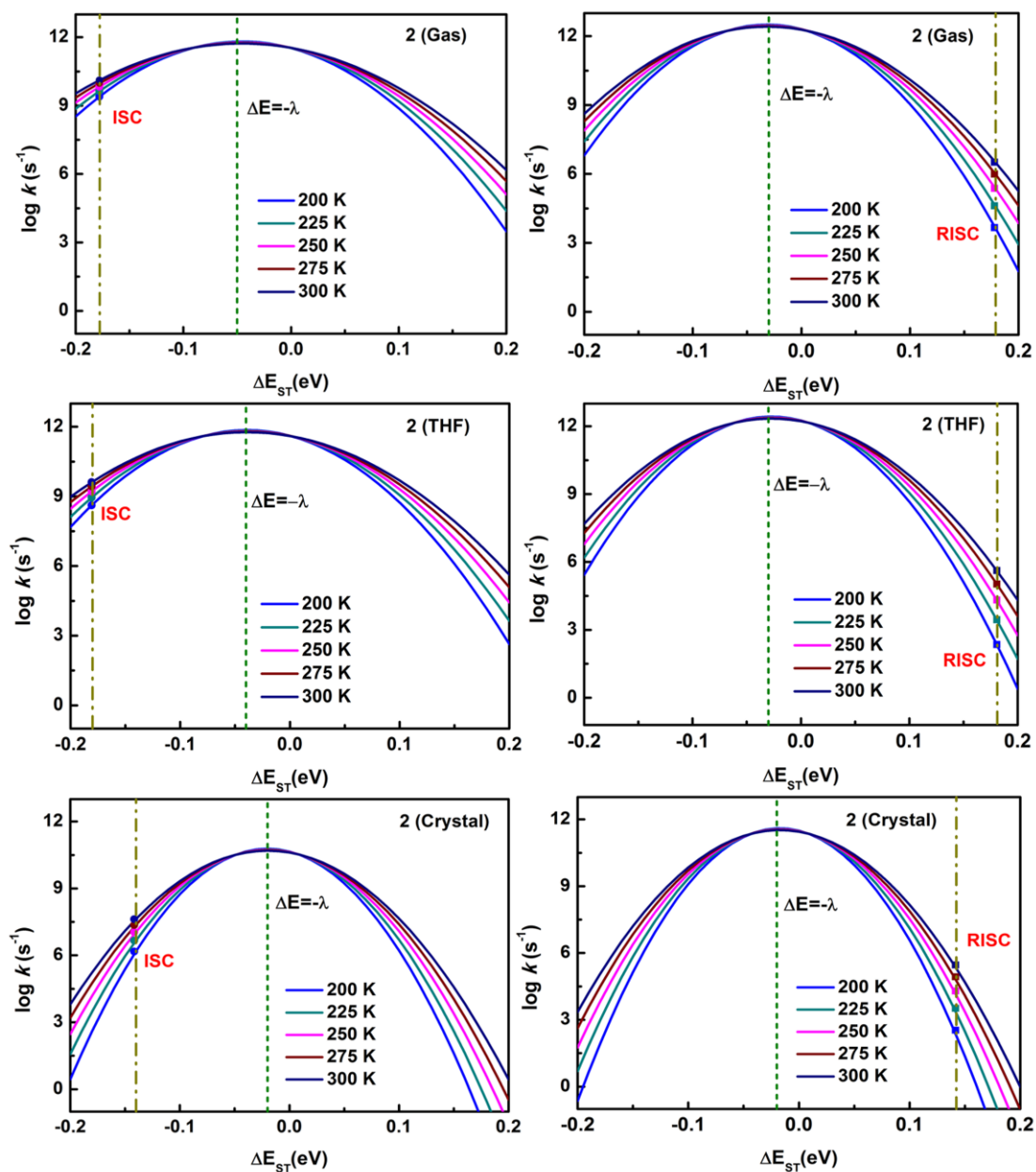


Figure S11. (R)ISC rate constant as a function of energy gap at different temperatures of **2** in gas, solution and crystal.

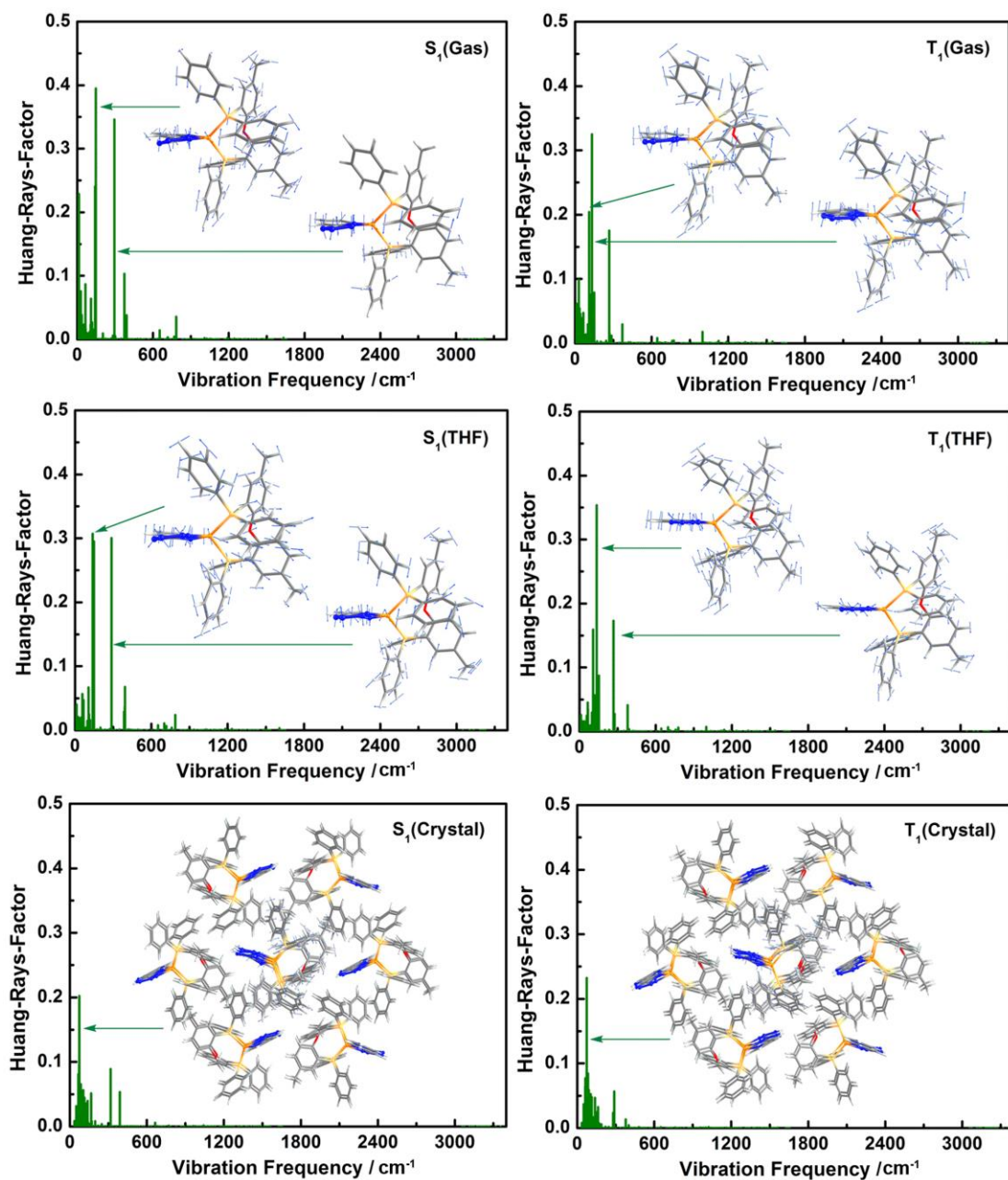


Figure S12. Huang-Rhys factors for energy conversion between S_1 and T_1 as well as displacement vectors of important vibration modes with the largest value of Huang-Rhys factor in gas, solution and crystal for **2**.

Table S3. Relative Energies (eV) of B3LYP/6-31G*&LANL2DZ (Cu) Optimized Structures for **1** and **2** in the Gas Phase, Solution, and Crystal. (Ground State Energy as Reference Point).

		Gas	Solution	Crystal
1	S₀	0	0	0
	S₁	2.91	2.95	2.92
	T₁	2.73	2.77	2.77
	$\Delta E_{S_1-T_1}$	0.18	0.18	0.15
2	S₀	0	0	0
	S₁	2.89	2.96	3.00
	T₁	2.72	2.78	2.86
	$\Delta E_{S_1-T_1}$	0.18	0.18	0.14

			At S₀	At S₁	At T₁
Gas	1	S₁	3.63	2.91	2.94
		T₁	3.23	2.75	2.73
		T₂	3.45	3.63	3.60
	2	S₁	3.62	2.89	2.93
		T₁	3.23	2.74	2.71
		T₂	3.43	3.63	3.60
Solution	1	S₁	3.66	2.95	3.00
		T₁	3.36	2.80	2.77
		T₂	3.44	3.72	3.67
	2	S₁	3.64	2.96	3.01
		T₁	3.36	2.81	3.01
		T₂	3.44	3.76	3.69
Crystal	1	S₁	3.49	2.90	2.92
		T₁	3.25	2.75	2.73
		T₂	3.30	3.52	3.43
	2	S₁	3.61	2.99	2.99
		T₁	3.30	2.86	2.84
		T₂	3.35	3.36	3.30

Table S4. Spin-Orbit Coupling Matrix Elements (SOCMEs) Values (cm⁻¹), Marcus Reorganization Energy (λ_{reorg} eV) Intersystem Crossing Rates and Reverse Intersystem Crossing Rates (s⁻¹) (ISC from S₁ to T₁ and RISC from T₁ to S₁).

		SOCMEs	$k_{\text{isc}}/k_{\text{risc}}$	λ_{reorg}
Gas		At S₁		
	1	21.48	8.03×10 ⁹	0.04
	2	21.03	1.30×10 ¹⁰	0.05
		At T₁		
	1	40.18	8.36×10 ⁵	0.03
	2	40.13	3.22×10 ⁶	0.03
Solution		At S₁		
	1	20.25	9.86×10 ⁹	0.04
	2	21.29	4.10×10 ⁹	0.04
		At T₁		
	1	36.81	1.87×10 ⁶	0.03
	2	37.28	4.17×10 ⁵	0.03
Crystal		At S₁		
	1	17.39	1.32×10 ⁹	0.03
	2	5.22	4.18×10 ⁷	0.02
		At T₁		
	1	36.65	2.08×10 ⁵	0.02
	2	12.97	2.93×10 ⁵	0.02

Compound 2	$\langle S_1 \hat{H}_{so} T_I \rangle$	$\langle S_1 \hat{H}_{so} T_{II} \rangle$	$\langle S_1 \hat{H}_{so} T_{III} \rangle$	$\Sigma(\text{SOMEs})^2$	Rates(s ⁻¹)
Gas					
ISC	11.89	12.26	12.26	442	1.30×10 ¹⁰
rISC	19.38	24.85	24.85	1611	3.22×10 ⁶
Solution					
ISC	12.68	12.10	12.10	453	4.10×10 ⁹
rISC	19.85	22.32	22.32	1390	4.17×10 ⁵
Crystal					
ISC	2.34	3.30	3.30	27	4.18×10 ⁷
rISC	0.31	9.17	9.17	168	2.93×10 ⁵

Table S5. The Temperature Dependence of the Intersystem Crossing Rates and Reverse Intersystem Crossing Rates (s⁻¹) (ISC from S₁ to T₁ and rISC form T₁ to S₁).

	Temperature (K)	<i>k_{ISC}</i>		
		Gas	Solution	Crystal
1	200	1.15×10 ⁹	1.69×10 ⁹	8.55×10 ⁶
	225	2.21×10 ⁹	3.07×10 ⁹	2.15×10 ⁸
	250	3.72×10 ⁹	4.92×10 ⁹	4.47×10 ⁸
	275	5.67×10 ⁹	7.20×10 ⁹	8.10×10 ⁸
	300	8.03×10 ⁹	9.86×10 ⁹	1.32×10 ⁹
2	200	2.50×10 ⁹	4.18×10 ⁸	1.48×10 ⁶
	225	4.37×10 ⁹	9.03×10 ⁸	4.55×10 ⁶
	250	6.81×10 ⁹	1.66×10 ⁹	1.11×10 ⁷
	275	9.73×10 ⁹	2.72×10 ⁹	2.29×10 ⁷
	300	1.30×10 ¹⁰	4.10×10 ⁹	4.18×10 ⁷
	Temperature (K)	<i>k_{rISC}</i>		
		Gas	Solution	Crystal
1	200	5.85×10 ²	2.22×10 ³	7.20×10 ¹
	225	6.64×10 ³	2.11×10 ⁴	1.04×10 ³
	250	4.62×10 ⁴	1.28×10 ⁵	8.68×10 ³
	275	2.25×10 ⁵	5.53×10 ⁵	4.92×10 ⁴
	300	8.36×10 ⁵	1.87×10 ⁶	2.08×10 ⁵
2	200	4.62×10 ³	2.24×10 ²	3.39×10 ²
	225	4.13×10 ⁴	2.78×10 ³	3.26×10 ³
	250	2.37×10 ⁵	2.07×10 ⁴	1.98×10 ⁴
	275	9.84×10 ⁵	1.07×10 ⁵	8.63×10 ⁴
	300	3.22×10 ⁶	4.17×10 ⁵	2.93×10 ⁵

Table S6. Oscillator Strength [T_1 ($f_{S_0-T_1}$) and S_1 ($f_{S_0-S_1}$)], Emission Rate Constant ($k_r^{P/F}/s^{-1}$) and lifetime ($\tau^{P/F}/\mu s$).

		Gas	Solution	Crystal
1	$f_{S_0-T_1,av}^a$	1.90×10^{-5}	1.35×10^{-5}	2.15×10^{-5}
	$k_{r,av}^P$	3.45×10^3	2.50×10^3	4.51×10^3
	$\tau_{r,av}^P$	290	401	222
	$f_{S_0-S_1}$	7.20×10^{-3}	1.63×10^{-2}	7.00×10^{-3}
	k_r^F	1.43×10^6	3.32×10^6	1.58×10^6
	τ_r^F	0.70	0.30	0.63
2	$f_{S_0-T_1,av}^a$	7.99×10^{-6}	1.32×10^{-5}	2.69×10^{-5}
	$k_{r,av}^P$	1.44×10^3	2.45×10^3	6.31×10^3
	$\tau_{r,av}^P$	694	409	158
	$f_{S_0-S_1}$	7.20×10^{-3}	1.70×10^{-2}	4.30×10^{-3}
	k_r^F	1.41×10^6	3.43×10^6	1.11×10^6
	τ_r^F	0.71	0.29	0.90

^a: The oscillator strength evaluated using the second-order perturbation theory based on relativistic scalar ZORA results obtained using the ADF program.

^b: k_r is evaluated by $k_r^{F/P} = \frac{2\pi\nu^2 e^2}{\epsilon_0 m c^3} f_{S_1, or T_1 \rightarrow S_0}$

Table S7. Vertical Excitation Energies (E_{\perp} , eV), Oscillator Strengths (f), Wavelength (nm) and Singly Occupied Orbitals Involved in the $S_0 \rightarrow S_n$ Electronic Transitions in the Gas Phase, Solution, and Crystal, Which are Computed by TD-B3LYP.

Gas					
		E_{\perp} (eV)	λ (nm)	Assignments	
1	S_1	3.63 (0.0179)	342	HOMO-1 \rightarrow LUMO (57.2)	MLCT +ILCT
				HOMO \rightarrow LUMO (38.4)	MLCT +ILCT
	S_2	3.73 (0.0625)	332	HOMO-1 \rightarrow LUMO (37.3)	MLCT +ILCT
				HOMO \rightarrow LUMO (59.1)	MLCT +ILCT
	S_3	3.80 (0.0163)	326	HOMO \rightarrow LUMO+1 (97.2)	MLCT +ILCT
	S_4	3.99 (0.0142)	311	HOMO \rightarrow LUMO+2 (84.9)	MLCT +ILCT
	S_5	4.03 (0.0054)	308	HOMO-1 \rightarrow LUMO+1 (71.3)	MLCT +ILCT
	S_6	4.04 (0.0126)	307	HOMO-3 \rightarrow LUMO (65.0)	MLCT +ILCT
	S_7	4.12 (0.0311)	301	HOMO \rightarrow LUMO+3 (82.1)	MLCT +ILCT
	...				
	S_{18}	4.39 (0.0005)	282	HOMO-2 \rightarrow LUMO+1 (84.3)	ILCT
	S_{19}	4.51 (0.0244)	275	HOMO \rightarrow LUMO+7 (45.0)	MLCT +ILCT
	S_{20}	4.51 (0.0346)	275	HOMO \rightarrow LUMO+8 (64.9)	MLCT +ILCT
	S_{21}	4.53 (0.0080)	273	HOMO-3 \rightarrow LUMO+2 (38.0)	MLCT +ILCT
				HOMO \rightarrow LUMO+7 (37.4)	MLCT +ILCT
	S_{22}	4.58 (0.0009)	271	HOMO-6 \rightarrow LUMO (88.6)	$n\pi^*$
	S_{23}	4.58 (0.0059)	270	HOMO-1 \rightarrow LUMO+6 (59.8)	MLCT +ILCT
	S_{24}	4.59 (0.0125)	270	HOMO-2 \rightarrow LUMO+2 (71.3)	ILCT
	S_{25}	4.60 (0.0006)	269	HOMO-3 \rightarrow LUMO+3 (54.5)	MLCT +ILCT

2	S₂₆	4.63	(0.0210)	268	HOMO-2 → LUMO+3 (53.1)	ILCT	
	S₂₇	4.67	(0.0067)	266	HOMO-3 → LUMO+4 (28.2)	MLCT +ILCT	
					HOMO → LUMO+9 (35.1)	MLCT +ILCT	
	S₂₈	4.68	(0.0288)	265	HOMO-3 → LUMO+5 (14.7)	MLCT +ILCT	
					HOMO-2 → LUMO+3 (14.7)	ILCT	
					HOMO-2 → LUMO+4 (15.2)		
					HOMO-1 → LUMO+9 (21.9)	MLCT +ILCT	
	S₂₉	4.70	(0.0097)	264	HOMO-2 → LUMO+3 (14.5)	ILCT	
					HOMO-2 → LUMO+4 (13.2)		
					HOMO → LUMO+9 (11.5)	MLCT +ILCT	
	S₃₀	4.71	(0.0001)	263	HOMO-1 → LUMO+7 (42.3)	MLCT +ILCT	
			E_⊥ (eV)		λ (nm)	Assignments	
	S₁	3.62	(0.0138)	343	HOMO-1 → LUMO (66.2)	MLCT +ILCT	
HOMO → LUMO (29.2)					MLCT +ILCT		
S₂	3.71	(0.0669)	334	HOMO-1 → LUMO (28.1)	MLCT +ILCT		
				HOMO → LUMO (68.3)	MLCT +ILCT		
S₃	3.79	(0.0166)	327	HOMO → LUMO+1 (68.3)	MLCT +ILCT		
S₄	4.00	(0.0014)	310	HOMO-3 → LUMO (53.6)	MLCT +ILCT		
S₅	4.01	(0.005)	309	HOMO-1 → LUMO+1 (65.9)	MLCT +ILCT		
S₆	4.03	(0.0323)	308	HOMO → LUMO+2 (62.9)	MLCT +ILCT		
S₇	4.12	(0.0273)	301	HOMO → LUMO+3 (80.2)	MLCT +ILCT		
...							
S₁₉	4.50	(0.0244)	276	HOMO → LUMO+7 (46.6)	MLCT +ILCT		
S₂₀	4.51	(0.022)	275	HOMO → LUMO+8 (70.6)	MLCT +ILCT		
S₂₁	4.54	(0.0091)	273	HOMO-3 → LUMO+2 (49.8)	MLCT		

						+ILCT
	S₂₂	4.57	(0.0043)	271	HOMO-6 → LUMO (61.8)	nπ*
	S₂₃	4.57	(0.0056)	271	HOMO-5 → LUMO+1 (46.6)	ILCT
	S₂₄	4.59	(0.0045)	270	HOMO-3 → LUMO+3 (53.3)	MLCT +ILCT
	S₂₅	4.61	(0.0234)	269	HOMO-2 → LUMO+2 (51.3)	ILCT
	S₂₆	4.63	(0.0101)	268	HOMO-2 → LUMO+6 (52.4)	ILCT
	S₂₇	4.64	(0.0074)	267	HOMO-2 → LUMO+3 (30.3)	ILCT
	S₂₈	4.66	(0.013)	266	HOMO-3 → LUMO+4 (29.9)	MLCT +ILCT
Solution						
		E_⊥ (eV)		λ (nm)	Assignments	
1	S₁	3.66	(0.0852)	339	HOMO-1 → LUMO (7.6)	MLCT +ILCT
					HOMO → LUMO (88.8)	MLCT +ILCT
	S₂	3.75	(0.0140)	331	HOMO-2 → LUMO (14.0)	MLCT +ILCT
					HOMO-1 → LUMO (75.3)	
	S₃	3.96	(0.0206)	313	HOMO → LUMO+1 (94.6)	MLCT +ILCT
	S₄	3.97	(0.0057)	312	HOMO-2 → LUMO (77.4)	MLCT +ILCT
	S₅	4.10	(0.0629)	303	HOMO → LUMO+2 (94.3)	MLCT +ILCT
	...					
	S₁₁	4.42	(0.0709)	281	HOMO-3 → LUMO (54.2)	ππ*+ILCT
	S₁₂	4.42	(0.0120)	280	HOMO-1 → LUMO+2 (21.9)	MLCT ILCT
					HOMO-1 → LUMO+3 (26.9)	MLCT +ILCT
	S₁₃	4.46	(0.0613)	278	HOMO-2 → LUMO+1 (84.4)	MLCT +ILCT
	S₁₄	4.51	(0.0400)	275	HOMO → LUMO+6 (84.5)	MLCT +ILCT
	S₁₅	4.55	(0.0106)	272	HOMO-1 → LUMO+3 (34.0)	MLCT +ILCT
					HOMO-1 → LUMO+4 (41.3)	
	S₁₆	4.57	(0.0268)	271	HOMO-2 → LUMO+2 (46.2)	MLCT +ILCT
					HOMO-1 → LUMO+4 (25.9)	
	S₁₇	4.61	(0.0395)	269	HOMO → LUMO+7 (41.8)	MLCT +ILCT
HOMO → LUMO+8 (45.3)						
S₁₈	4.62	(0.0065)	269	HOMO-1 → LUMO+5 (62.0)	MLCT +ILCT	

	S₁₉	4.62	(0.0250)	268	HOMO-2 → LUMO+3 (52.1)	MLCT +ILCT
	S₂₀	4.64	(0.0066)	267	HOMO → LUMO+7 (30.0)	MLCT +ILCT
	S₂₁	4.66	(0.0008)	266	HOMO-7 → LUMO (57.7)	MLCT +ILCT
	S₂₂	4.70	(0.0218)	264	HOMO-2 → LUMO+4 (67.6)	MLCT +ILCT
	...					
	S₃₀	4.89	(0.0443)	254	HOMO-4 → LUMO+2 (54.4)	ILCT +ππ*
		E_⊥ (eV)		λ (nm)	Assignments	
2	S₁	3.64	(0.0867)	340	HOMO-1 → LUMO (6.9)	MLCT +ILCT
					HOMO → LUMO (89.9)	MLCT +ILCT
	S₂	3.73	(0.0130)	332	HOMO-1 → LUMO (74.9)	MLCT +ILCT
	S₃	3.95	(0.0049)	314	HOMO-2 → LUMO (73.6)	MLCT +ILCT
	S₄	3.97	(0.0230)	313	HOMO → LUMO+1 (96.7)	MLCT +ILCT
	S₅	4.10	(0.0654)	303	HOMO → LUMO+2 (94.4)	MLCT +ILCT
	...					
	S₁₁	4.41	(0.0729)	281	HOMO-4 → LUMO (54.7)	ππ*+ILCT
	S₁₂	4.43	(0.0136)	280	HOMO-1 → LUMO+2 (33.1)	MLCT +ILCT
					HOMO-1 → LUMO+3 (33.4)	
	S₁₃	4.46	(0.0624)	278	HOMO-2 → LUMO+1 (84.2)	MLCT +ILCT
	S₁₄	4.52	(0.0038)	275	HOMO-3 → LUMO (70.2)	ILCT
	S₁₅	4.54	(0.0297)	273	HOMO-2 → LUMO+2 (31.2)	MLCT +ILCT
	S₁₆	4.55	(0.0243)	273	HOMO-1 → LUMO+4 (44.2)	MLCT +ILCT
HOMO → LUMO+6 (29.0)					MLCT +ILCT	
S₁₇	4.56	(0.0269)	272	HOMO-1 → LUMO+4 (25.1)	MLCT +ILCT	
				HOMO → LUMO+6 (35.9)	MLCT +ILCT	
S₁₈	4.60	(0.0174)	270	HOMO → LUMO+7 (41.4)	MLCT	

					+ILCT
	S₁₉	4.61 (0.0065)	269	HOMO-1 → LUMO+5 (64.6)	MLCT +ILCT
	S₂₀	4.62 (0.0232)	269	HOMO → LUMO+8 (40.0)	MLCT +ILCT
	S₂₁	4.63 (0.0094)	268	HOMO-3 → LUMO+1 (51.4)	ILCT
	S₂₂	4.64 (0.0129)	267	HOMO → LUMO+8 (30.3)	MLCT +ILCT
Crystal					
		E_⊥ (eV)	λ (nm)	Assignments	
1	S₁	3.49 (0.0460)	355	HOMO-1 → LUMO (11.4)	MLCT +ILCT
				HOMO → LUMO (78.6)	MLCT +ILCT
	S₂	3.69 (0.0282)	336	HOMO-1 → LUMO (68.1)	MLCT +ILCT
	S₃	3.83 (0.0159)	324	HOMO → LUMO+1 (78.1)	MLCT +ILCT
	S₄	3.84 (0.0111)	322	HOMO-2 → LUMO (59.3)	MLCT +ILCT
	S₅	4.02 (0.0041)	308	HOMO → LUMO+3 (59.8)	MLCT +ILCT
	...				
	S₁₃	4.40 (0.0118)	282	HOMO-1 → LUMO+2 (58.0)	MLCT +ILCT
	S₁₄	4.42 (0.0015)	280	HOMO-5 → LUMO (63.9)	nπ*
	S₁₅	4.43 (0.0063)	280	HOMO-5 → LUMO (25.5)	nπ*
				HOMO-2 → LUMO+3 (25.8)	MLCT +ILCT
	S₁₆	4.48 (0.0132)	277	HOMO-2 → LUMO+2 (36.5)	MLCT +ILCT
				HOMO → LUMO+6 (30.0)	
	S₁₇	4.49 (0.0036)	276	HOMO-1 → LUMO+4 (43.9)	MLCT +ILCT
	S₁₈	4.50 (0.0317)	276	HOMO-1 → LUMO+4 (31.9)	MLCT +ILCT
				HOMO → LUMO+6 (43.3)	MLCT +ILCT
S₁₉	4.52 (0.0121)	274	HOMO → LUMO+7 (60.5)	MLCT +ILCT	
S₂₀	4.56 (0.0042)	272	HOMO → LUMO+8 (70.0)	MLCT +ILCT	
S₂₁	4.57 (0.0079)	271	HOMO-4 → LUMO (86.8)	ILCT	

	S₂₂	4.60	(0.0306)	269	HOMO-2 → LUMO+4 (45.3)	MLCT +ILCT
	S₂₃	4.62	(0.0079)	268	HOMO-4 → LUMO+1 (46.7)	ILCT
	S₂₄	4.64	(0.0041)	267	HOMO-3 → LUMO+1 (78.2)	ILCT
	S₂₅	4.67	(0.0003)	266	HOMO-10 → LUMO (42.7)	ILCT +nπ*
	S₂₆	4.67	(0.0025)	265	HOMO → LUMO+9 (56.2)	MLCT +ILCT
		E_⊥ (eV)		λ (nm)	Assignments	
2	S₁	3.54	(0.0358)	351	HOMO-1 → LUMO (14.8)	MLCT +ILCT
					HOMO → LUMO (76.7)	MLCT +ILCT
	S₂	3.61	(0.0154)	343	HOMO-1 → LUMO (74.2)	MLCT +ILCT
	S₃	3.86	(0.0268)	321	HOMO-2 → LUMO (80.5)	MLCT +ILCT
	S₄	3.90	(0.0092)	318	HOMO → LUMO+1 (95.9)	MLCT +ILCT
	S₅	4.04	(0.039)	307	HOMO → LUMO+2 (88.4)	MLCT +ILCT
	S₆	4.08	(0.0076)	304	HOMO → LUMO+3 (83.2)	MLCT +ILCT
	S₇	4.11	(0.0524)	302	HOMO → LUMO+4 (87.0)	MLCT +ILCT
	...					
	S₁₈	4.45	(0.0246)	279	HOMO-2 → LUMO+3 (30.1)	MLCT +ILCT
					HOMO → LUMO+6 (26.6)	
	S₁₉	4.47	(0.0409)	278	HOMO → LUMO+6 (49.5)	MLCT +ILCT
	S₂₀	4.48	(0.0096)	276	HOMO-3 → LUMO+1 (61.8)	ILCT
	S₂₁	4.52	(0.006)	274	HOMO-2 → LUMO+4 (34.2)	MLCT +ILCT
S₂₂	4.53	(0.0067)	274	HOMO → LUMO+8 (49.2)	MLCT +ILCT	
S₂₃	4.57	(0.0266)	271	HOMO-2 → LUMO+4 (41.3)	MLCT +ILCT	
S₂₄	4.64	(0.0151)	267	HOMO-3 → LUMO+4 (31.0)	ILCT	

Table S8. Vertical Emission Energies (E_{\perp} , eV), Oscillator Strengths (f), Wavelength (nm) and Singly Occupied Orbitals Involved in the $S_1 \rightarrow S_0$ and $T_1 \rightarrow S_0$ Electronic Transitions in the Gas Phase, Solution, and Crystal.

Gas						
		E_{\perp} (eV)		λ (nm)	Assignments	
1	S_1	2.14	(0.0072)	578	HOMO \rightarrow LUMO (97.9)	MLCT +ILCT
	T_1	2.05	(0.0000)	603	HOMO \rightarrow LUMO (96.9)	MLCT +ILCT
2	S_1	2.13	(0.0072)	583	HOMO \rightarrow LUMO (97.9)	MLCT +ILCT
	T_1	2.04	(0.0000)	609	HOMO \rightarrow LUMO (96.9)	MLCT +ILCT
Solution						
		E_{\perp} (eV)		λ (nm)	Assignments	
1	S_1	2.17	(0.0163)	571	HOMO \rightarrow LUMO (97.9)	MLCT +ILCT
	T_1	2.07	(0.0000)	599	HOMO \rightarrow LUMO (96.5)	MLCT +ILCT
2	S_1	2.16	(0.0170)	573	HOMO \rightarrow LUMO (97.8)	MLCT +ILCT
	T_1	2.07	(0.0000)	600	HOMO \rightarrow LUMO (96.4)	MLCT +ILCT
Crystal						
		E_{\perp} (eV)		λ (nm)	Assignments	
1	S_1	2.28	(0.0070)	545	HOMO \rightarrow LUMO (96.6)	MLCT +ILCT
	T_1	2.20	(0.0000)	564	HOMO \rightarrow LUMO (95.0)	MLCT +ILCT
2	S_1	2.44	(0.0043)	509	HOMO \rightarrow LUMO (94.1)	MLCT +ILCT
	T_1	2.33	(0.0000)	531	HOMO \rightarrow LUMO (90.0)	MLCT +ILCT

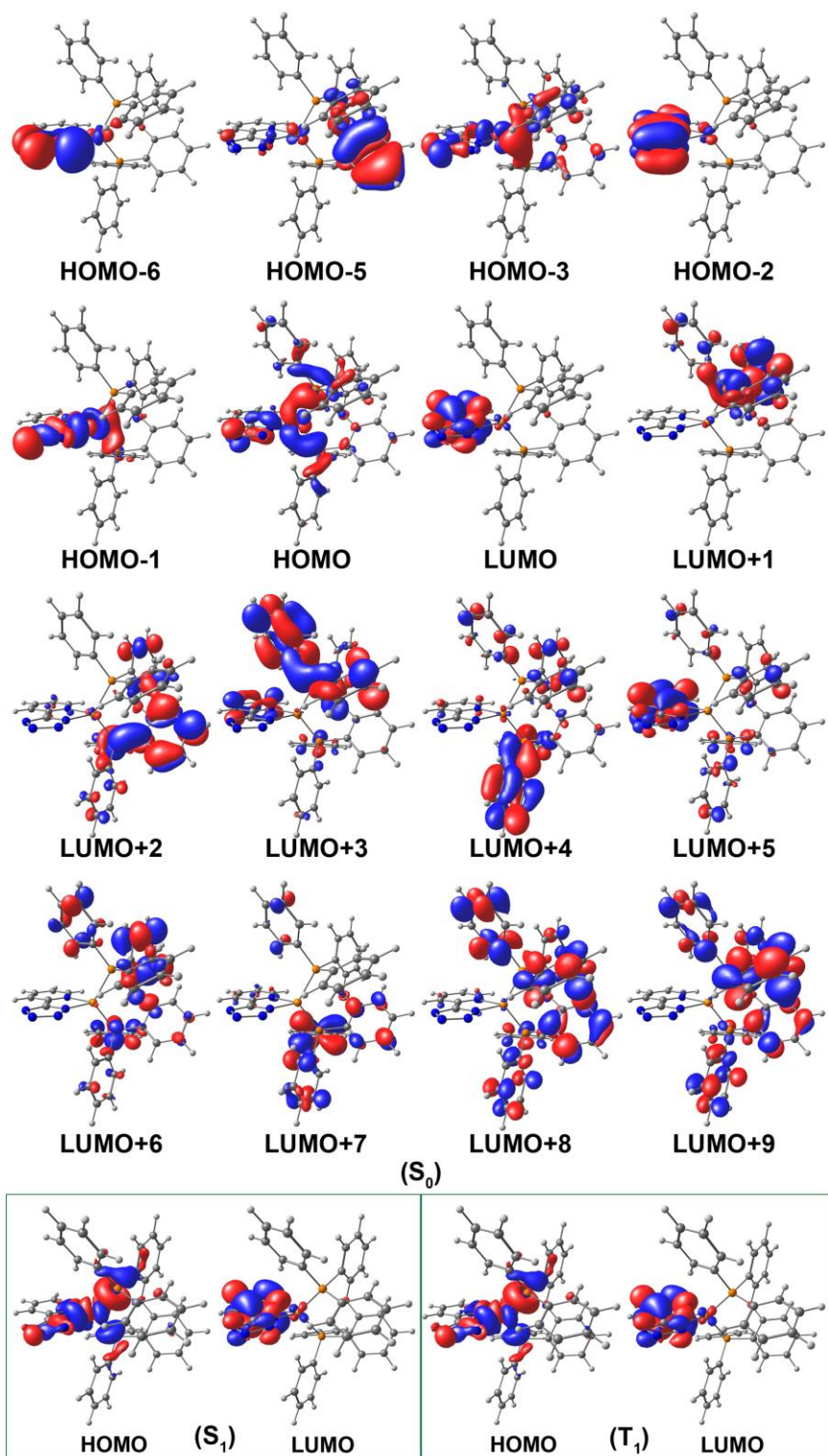


Figure S13. TD-DFT computed canonical molecular orbitals at the S₀, S₁ and T₁ minima of compound **1** in gas phase.

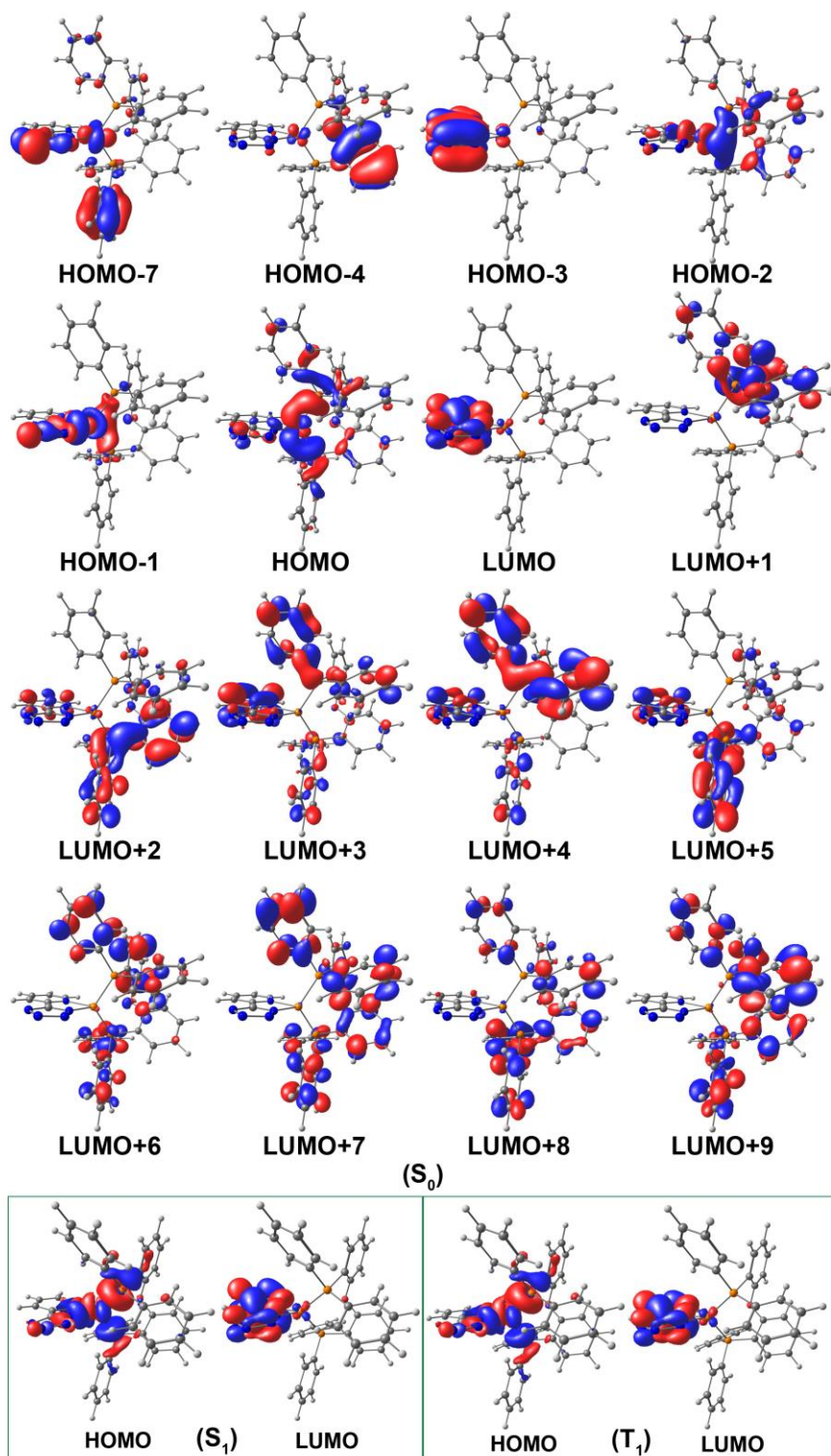


Figure S14. TD-DFT computed canonical molecular orbitals at the S₀, S₁ and T₁ minima of compound **1** in solution.

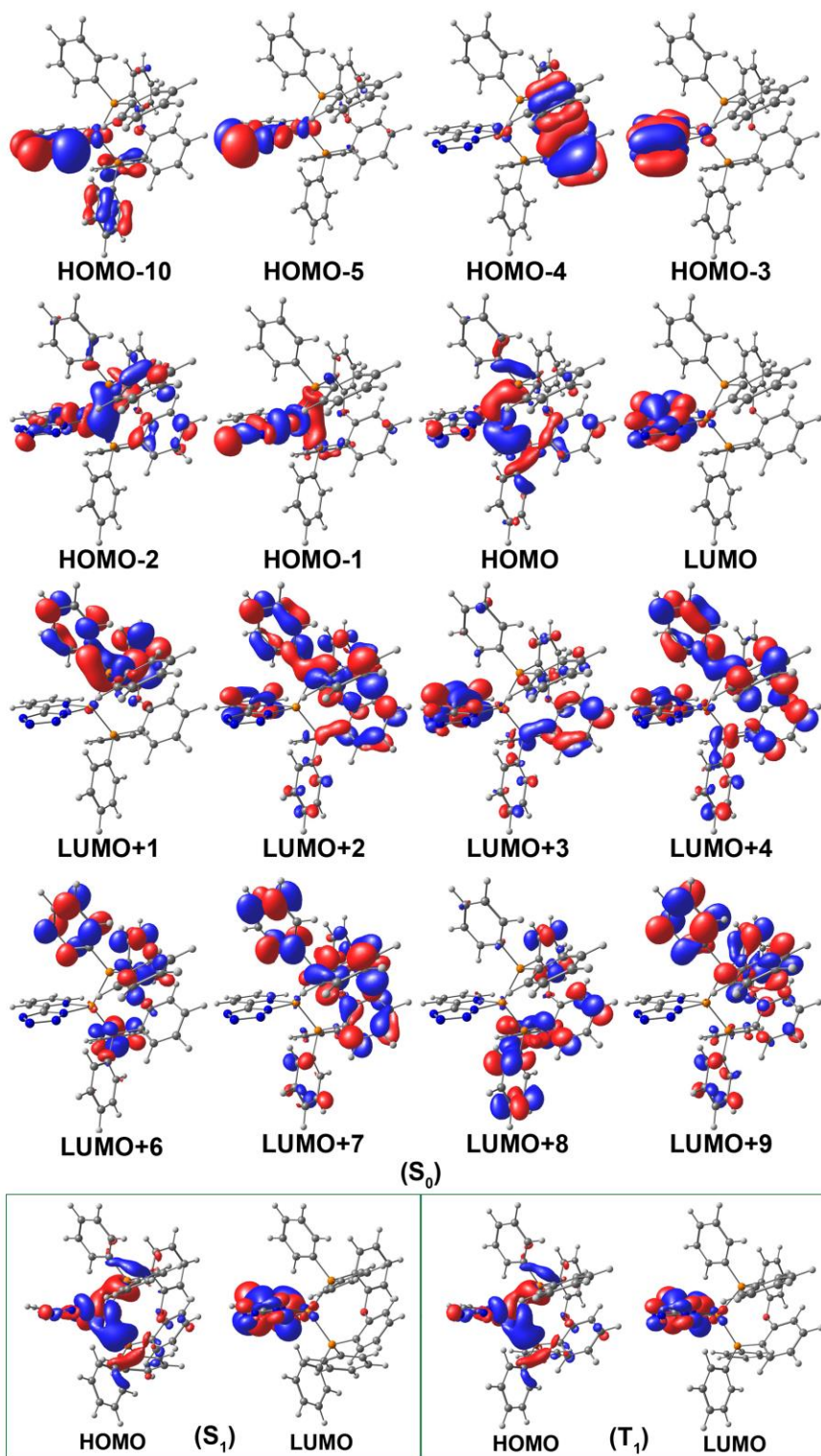


Figure S15. TD-DFT computed canonical molecular orbitals at the S₀, S₁ and T₁ minima of compound **1** in crystal.

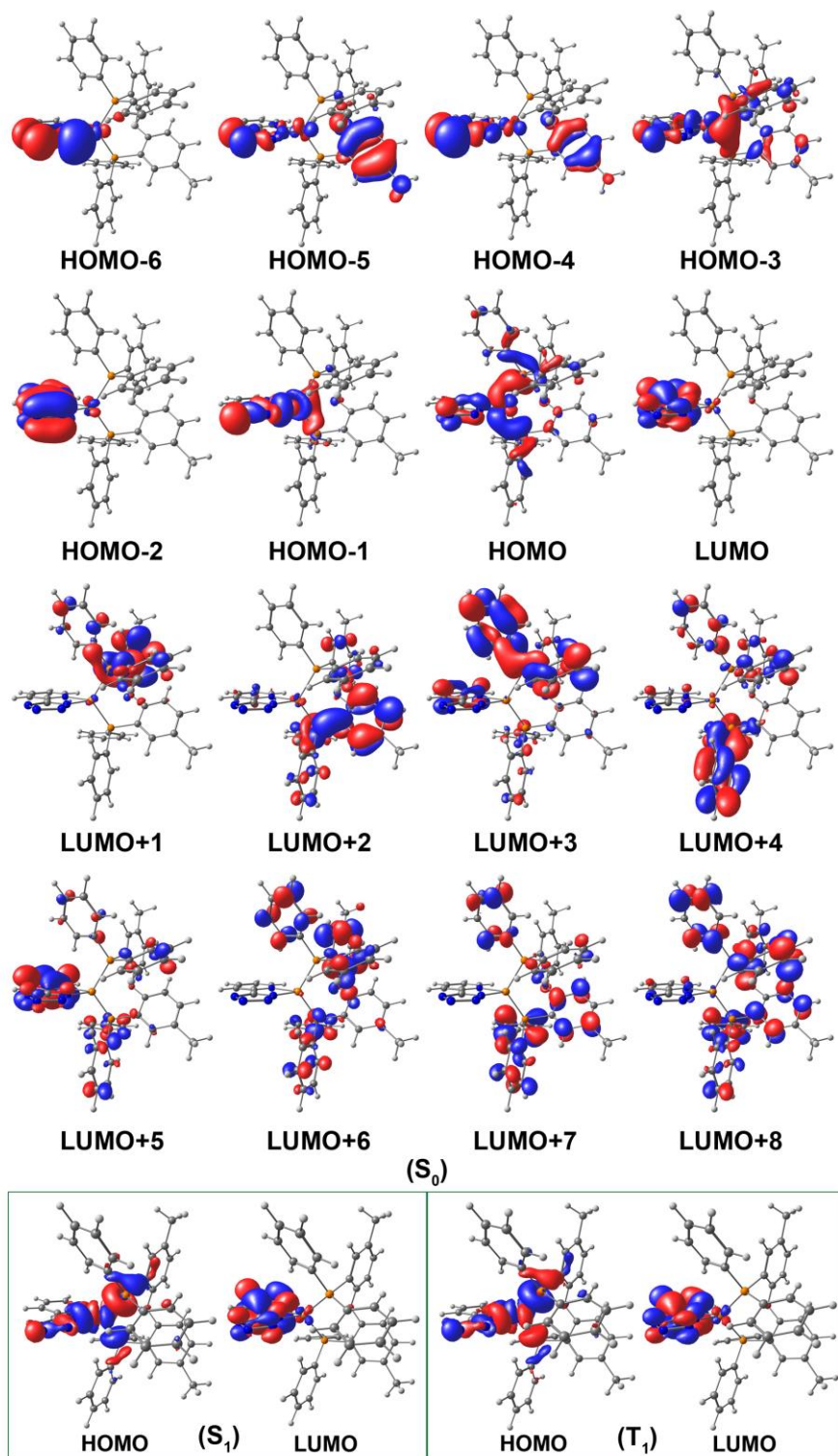


Figure S16. TD-DFT computed canonical molecular orbitals at the S₀, S₁ and T₁ minima of compound **2** in gas phase.

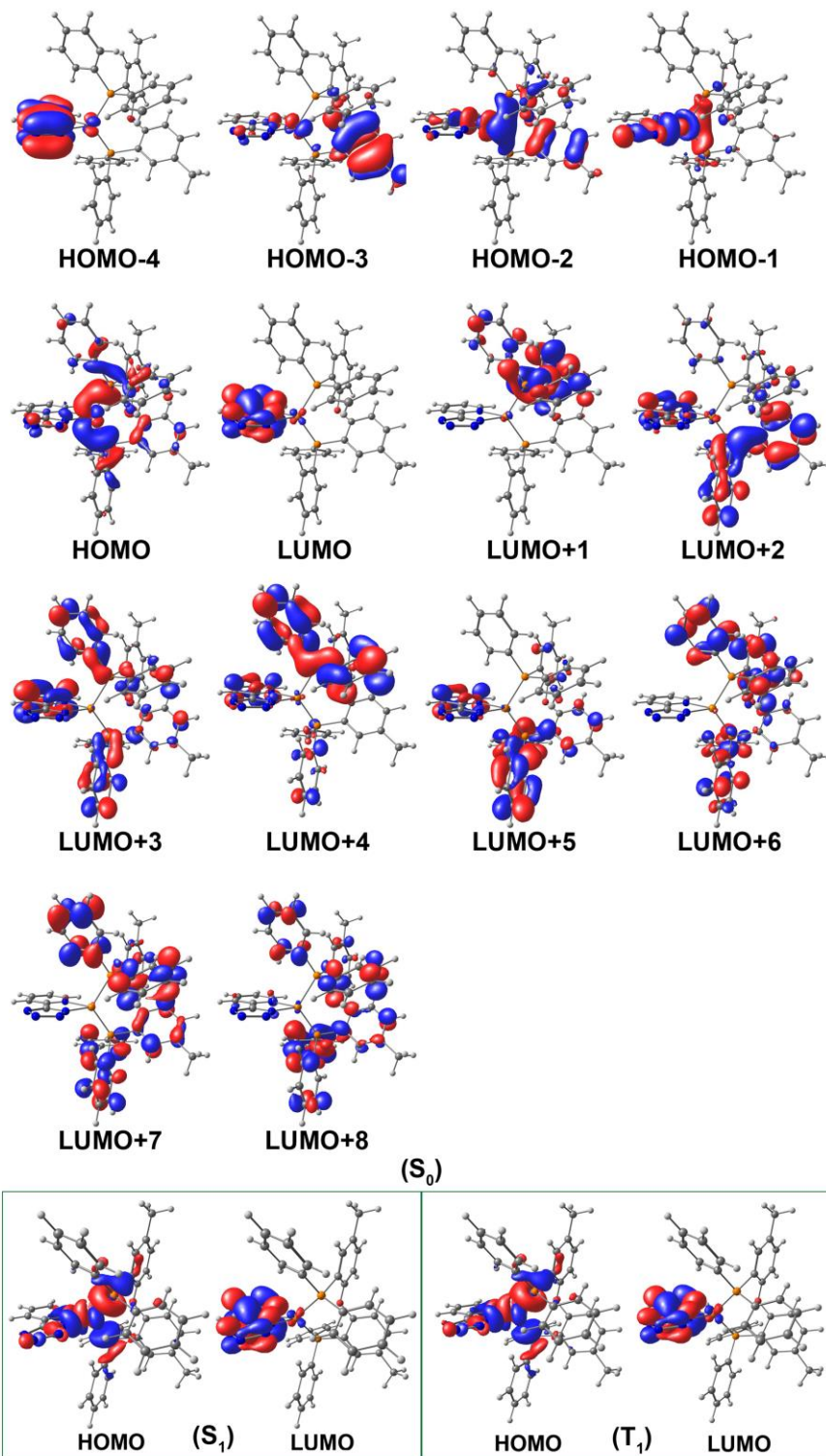


Figure S17. TD-DFT computed canonical molecular orbitals at the S₀, S₁ and T₁ minima of compound **2** in solution.

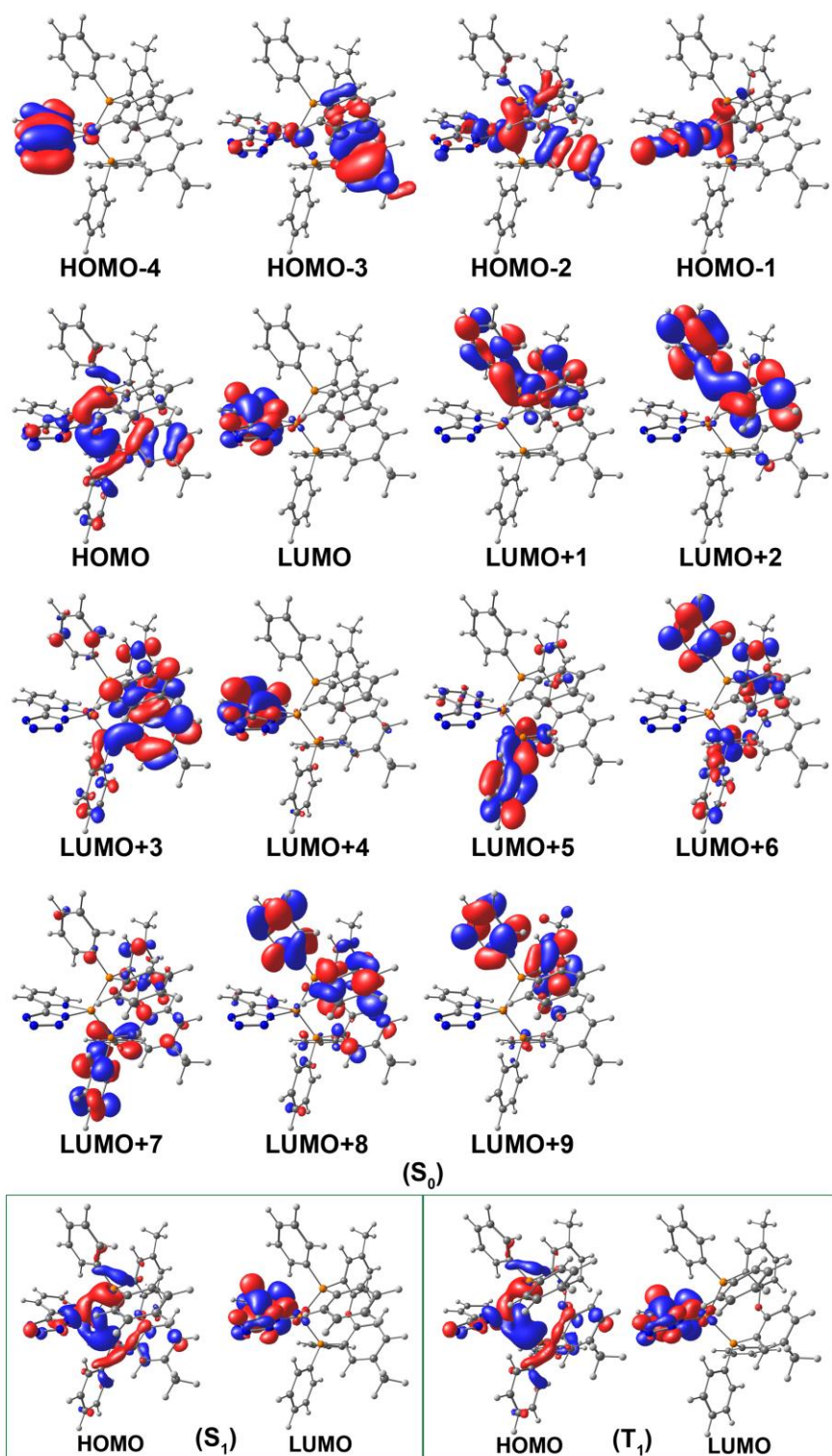


Figure S18. TD-DFT computed canonical molecular orbitals at the S₀, S₁ and T₁ minima of compound **2** in crystal.

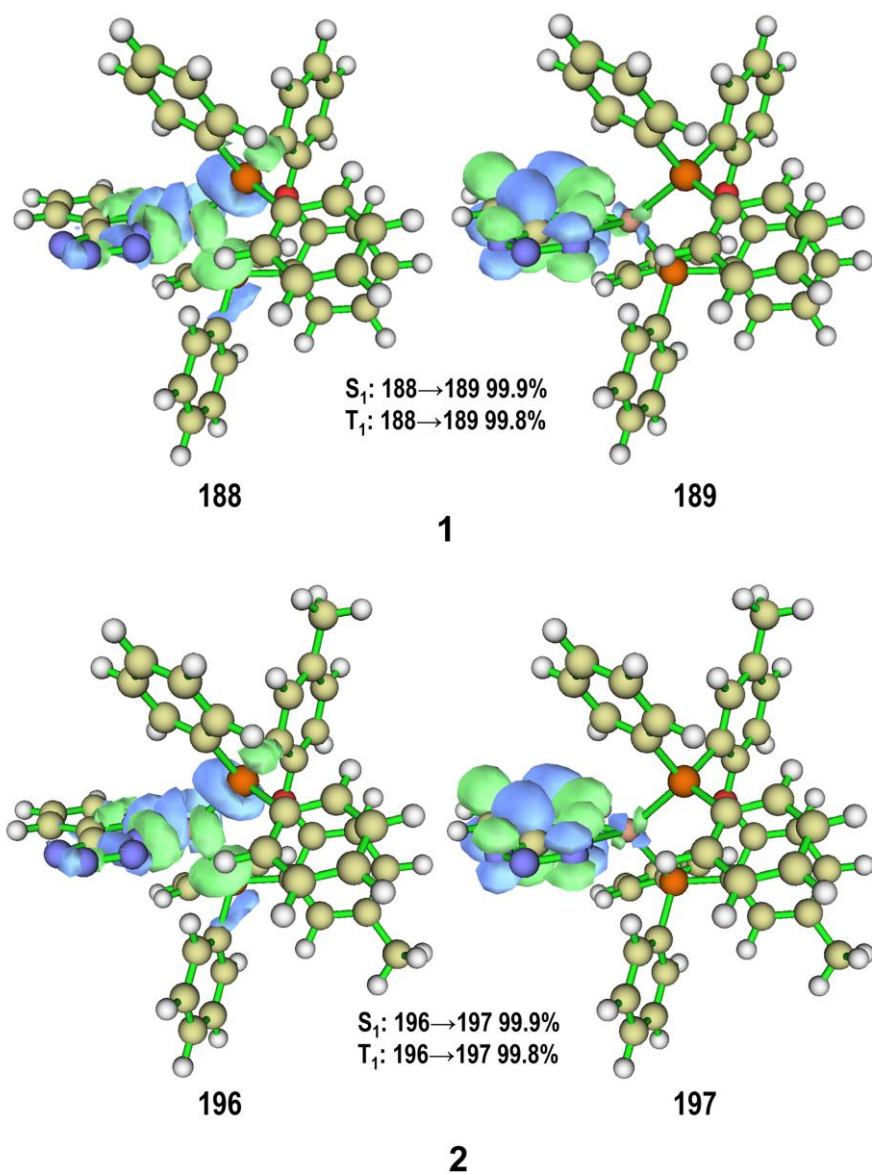


Figure S19. Natural transition orbital pairs at the S₁ and T₁ minima of compound **1** and **2** calculated using the Multiwfn package².

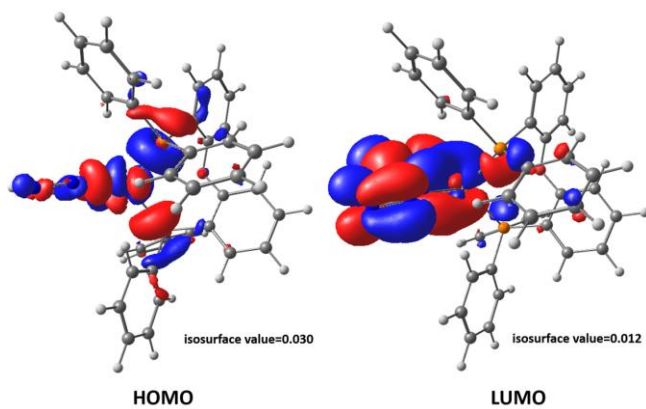


Figure S20. TD-DFT computed HOMO and LUMO at the S₁ minima of compound **1** in solution.

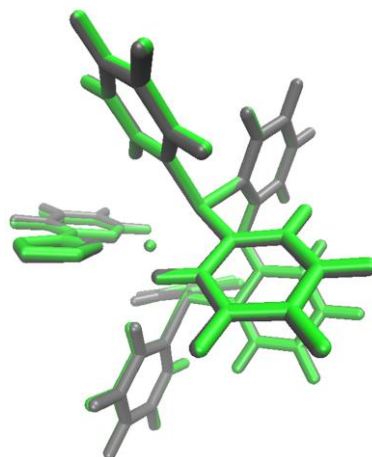


Figure S21. Overlays of S_1 (gray) and T_1 (green) structures in solution for complex **1**.

References

1. L. Bergmann, J. Friedrichs, M. Mydlak, T. Baumann, M. Nieger and S. Bräse, *Chem. Commun.* 2013, **49**, 6501.
2. T. Lu and F. Chen, *J. Comput. Chem.*, 2012, **33**, 580.